XLPE Cable Insulation Resistance Modelling under Annealing and Thermal Ageing Effects

Xufei Ge, Fulin Fan, Martin J. Given, and Brian G. Stewart
Institute for Energy and Environment, University of Strathclyde
204 George Street, Glasgow, G1 1XW, United Kingdom
xufei.ge@strath.ac.uk, f.fan@strath.ac.uk, m.given@strath.ac.uk, brian.stewart.100@strath.ac.uk

***Abstract*- Cross-linked polyethylene (XLPE) insulated electrical cables are widely deployed for electricity transmission due to the reliable thermomechanical performance and excellent electrical dielectric properties of XLPE insulation. Insulation resistance (IR) is a common metric indicating the electrical condition of cable insulation that undergoes annealing and thermal ageing over its service life. Most research related to the IR simulation deals with either the thermal ageing process of XLPE insulation itself or the annealing process of XLPE insulation by considering the diffusion of chemical specifies from semicon layers. This paper develops a discretisation IR model to estimate the temperature distribution across the XLPE insulation layer and simulate the IR drop under the thermal ageing effect or the U-shape variation of IR under the joint effects of annealing and thermal ageing, respectively. The IR simulation results are discussed around the necessity of combining annealing and thermal ageing effects for IR simulation with the presence of semicon layers.**

I. INTRODUCTION

The insulation of high- and medium-voltage electrical cables is usually made of polymers such as cross-linked polyethylene (XLPE) which has excellent electrical dielectric properties and reliable thermomechanical performance [1], [2]. Compared to other electricity transmission and conversion equipment, long-distance underground or submarine electrical cables generally receive less periodic maintenance, though the cable insulation is subjected to various stresses including electrical, chemical, thermal and mechanical stresses which can cause insulation degradation and eventually cable failures [3], [4]. Therefore, it is necessary to perform cable lifetime estimation to predict the remaining lifetime of the aged cable and supply a basis for preventative maintenance.

Insulation resistance (IR) measurements are one of the cable condition monitoring techniques that can most directly reflect on the cable condition [5]. By analysing the IR or conductivity measurements of cable samples degrading under different field or laboratory conditions, the roles of influencing factors in altering the IR or conductivity are widely investigated and simulated in literature. Particular attention has been paid to the thermal ageing that can distinctly change the insulation state of the XLPE cable operating at elevated temperature [6]. The gap between conduction and valence bands that indicates the energy required for electronic transition in XLPE insulation has been measured to drop with the thermal ageing time [7], illustrating that thermal ageing can reduce the IR when it is determined under the band conduction mechanism. The ageing temperature and the IR variation over time are connected in [8] by randomly dividing the XLPE insulation into degraded and non-degraded segments which possess disparate resistivity, with the volume ratio of the two parts being inferred from the ageing time and temperature. The sensitivity of the bulk IR to the segment size is further assessed in [9], finding that the resolution along the radial dimension dominating the surface current flow area has greater impacts on the IR. Even though the dichotomy models proposed in [8] and [9] are able to depict the long-term decline of IR with thermal ageing time, they assume the insulation layer is uniform in the ageing temperature and therefore select the degraded segments in a random way. In addition, they reflect the thermal ageing of the insulation itself without considering the diffusion of chemical species from semicon layers over the initial heating (or annealing) process. The defects associated with the chemical species will act as trapping centres of charges which promote hopping conduction and reduce the related IR [10]. In [10], the insulation conductivity measurements of XLPE cable samples annealed at 90 ℃ exhibit a hump shape over 90 days (i.e., implying a U-shape pattern of the IR), which is attributed to the cumulation and then exhaustion of the chemical species diffused from semicon layers. To that end, the hopping and band conduction mechanisms, i.e., two prevailing conduction mechanisms in XLPE insulation [11], should be combined in order to more accurately reflect the joint effects of annealing and thermal ageing on IR variations throughout the heating process with the presence of semicon layers.

This paper addresses the deficiency of the dichotomy model in previous work [9] by developing a discretisation IR model to simulate resistances of XLPE insulation segments that are aged at various temperatures. The temperature distribution across the insulation sample is interpolated by an artificial neural network trained based on the finite volume simulation. A temperature-related degradation rate is then used to calculate the resistivity decline and the resulting IR drop under thermal ageing effects. In addition, the joint effects of annealing and thermal ageing are modelled here by referring to the conductivity measurements of the XLPE insulation sample in contact with semicon layers over the heating process. The IR simulation results under the thermal ageing effect or under the joint effects of annealing and thermal ageing are compared and discussed around possible approaches to combining the two effects.

The paper is structured as follows: Section II describes the discretisation IR model with distributed temperature; Section III discusses the IR simulation results under the thermal ageing effect or joint effects of annealing and thermal ageing; Section IV gives conclusions and recommendations for further work.

II. Discretisation Insulation Resistance Model

A. Cable Temperature Simulation

Cable insulation generally has a non-uniform distribution of temperature along both radial and longitudinal dimensions due to the fact that power cables covering long distances cross various environment regions [12]. To facilitate the modelling of insulation degradation with distributed temperature, the cable insulation is divided here into a large number of small segments, as shown in Fig. 1(a). The scales of segments are determined by the resolutions adopted along radial, angular and longitudinal directions, denoted by Δx, $\Delta\varphi$ and Δl respectively, as shown in Fig. 1(b). An insulation layer sample with 1m length, 0.0075m inner radius and 0.0115m outer radius is modelled in this work with the resolutions Δx, $\Delta\varphi$ and Δl equalling 0.0004 m, 2° and 0.02 m respectively. This insulation layer sample is half of a 2m XLPE cable inside a chamber, the temperature within which is simulated by using a finite volume method (FVM) [13] with a power density of 103 kW/m^3 applied on the conductor core. Then an artificial neural network [13] is trained using the FVM-based temperature simulation and interpolates the temperature for all the segments, as shown in Fig. 2. Higher temperature generally occurs at the segments closer to the conductor core and/or the bottom of the 1m insulation sample which locates at the centre of the chamber.

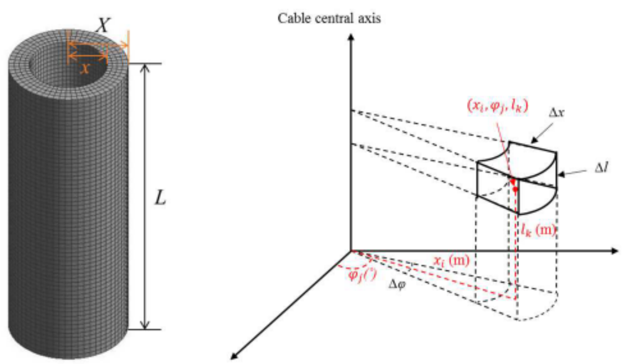

(a) (b)

Fig. 1. (a) Division of insulation layer into segments based on (b) the resolutions adopted along radial, angular and longitudinal dimensions.

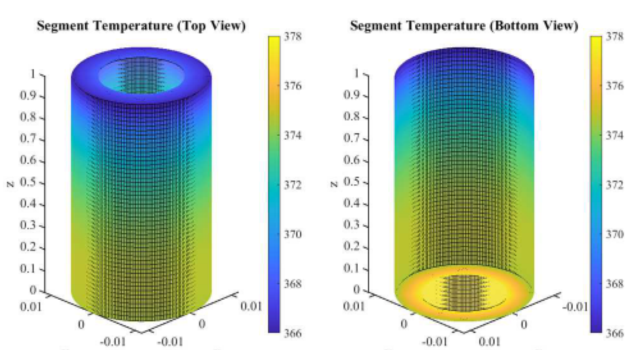

Fig. 2. The ageing temperature (K) distributed across insulation segments.

B. IR Model for Thermal Ageing Effect Only

A flow chart describing the discretisation IR model for thermal ageing is shown in Fig. 3. Given the temperature $T(x_i, \varphi_j, l_k)$ of the segment locating at the i^{th}, j^{th} and k^{th} units along radial, angular and longitudinal dimensions in combination with a degradation rate constant λ_0 and the activation energy E_a of the degradation reaction, the segment's degradation rate $\lambda(T)$ (in 1/day) is calculated by using the Arrhenius model [8]:

$$\ln(\lambda(T)) = \ln(\lambda_0) + \left(\frac{-E_a}{k_B}\right)\cdot\frac{1}{T} \tag{1}$$

Then the resistivity $\rho(t,T)$ of the segment aged at T over the heating time t (day) is estimated from its initial non-degraded resistivity $\rho_0(T)$ by (2) [8] and translated into the segment's resistance $R(t,T)$ by (3) based on the segment size [14].

$$\rho(t,T) = \rho_0(T)\cdot\exp(-\lambda(T)\cdot t) \tag{2}$$

$$R(t,T) = \frac{\rho(t,T)}{\Delta\varphi\cdot\Delta l}\cdot\ln\left(\frac{x_i+\frac{\Delta x}{2}}{x_i-\frac{\Delta x}{2}}\right) \tag{3}$$

Then the resistances of all the segments estimated via (1)-(3) at their respective T (see Fig. 2) over t are used to calculate the bulk IR $R_B(t)$ of the entire insulation under the thermal ageing. Specifically, the series resistance of the segments along each radial column is first computed given fixed angular and longitudinal units; and then the parallel resistance of all the radial columns is calculated as the bulk IR $R_B(t)$ [9].

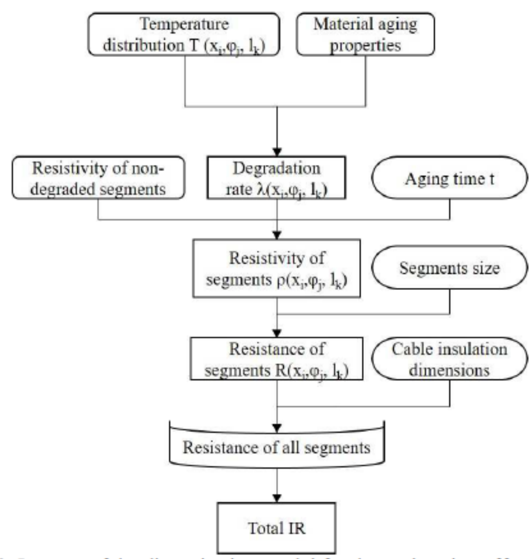

Fig. 3. Process of the discretisation model for thermal ageing effect only.

The resistivity measurements performed in [15] for the XLPE insulation samples subject to thermal ageing at 80 ºC, 100 ºC, 120 ºC or 140 ºC are used here to estimate the model parameters for the thermal ageing effect. (The reader is referred to Figure 3 in [15] for insulation resistivity measurements). Table I lists the temperature-dependent initial non-degraded resistivity ρ_0 and degradation rates λ that are extracted from initial resistivity measurements and fitted to the drop of resistivity with time, respectively [8]. The decrease of ρ_0 with T and the relationship between $\ln(\lambda)$ and $1/T$ are approximated here by linear fitting, from which model parameters are derived, as listed in Table II.

TABLE I
INITIAL NON-DEGRADED RESISTIVITY AND DEGRADATION RATES OF XLPE INSULATION AT FOUR AGEING TEMPERATURE LEVELS

Temperature	ρ_0 (Ω·m)	λ (1/day)
353 K (80 ℃)	2×10^{12}	2.04%
373 K (100 ℃)	1×10^{12}	2.4%
393 K (120 ℃)	3.2×10^{11}	21.6%
413 K (140 ℃)	1.95×10^{11}	33.6%

TABLE II
DISCRETISATION IR MODEL PARAMETERS FOR THERMAL AGEING

Parameter	Unit	Value
λ_0	1/day	$4.37 \times 10^{9}\%$
E_a	kJ	64
$\rho_0(T)$	Ω·m	$(-3.0475 \cdot T + 1289) \times 10^{10}$

C. IR Model for Joint Effects of Annealing & Thermal Ageing

The discretisation model for the joint effects of annealing and thermal ageing calculates the bulk IR from segment resistivity in the same way as depicted in Fig. 3, but estimates the segment resistivity variation with time by referring to the conductivity of XLPE insulation samples measured over the heating process with the presence of semicon layers [11]. Fig. 4(a) shows the insulation conductivity σ (S/m) of XLPE cable samples measured in [11] when they were heated at 90 ℃ over different durations. The hump shape of σ is mainly caused by the cumulation and then exhaustion of chemical species diffused from semicon layers which enhance hopping conduction. Through fitting a gamma distribution (Γ) based function to σ measurements, the variation of σ with t at 90 ℃ under the joint effects of annealing and thermal ageing is approximated by (4), as shown in Fig. 4(a). It is noted that cross-linking by-products created in manufacturing can also promote hopping conduction and thus raise the initial σ. When these by-products along with the chemical species are exhausted after a sufficient long duration, the resulting σ (e.g., at 90 days) might be even smaller than the initial σ.

$$\sigma(t, 90℃) = 9.31 \cdot 10^{-15} + 3.26 \cdot 10^{-13} \cdot \Gamma\left(\frac{(t+20.55)}{1.179}; 13.65, 3.17\right) \quad (4)$$

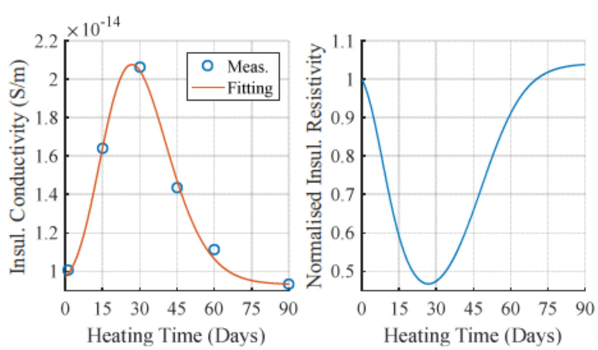

(a) (b)

Fig. 4. (a) Insulation conductivity measurements and their fitted values (S/m) of XLPE insulation samples heated at 90 ℃ over various durations (days) with the presence of semicon layers and (b) the corresponding insulation resistivity normalised by the initial level.

Given the reciprocal relationship of σ and ρ, the variation of insulation resistivity normalised by the initial level is inferred from the fitting of σ, as shown in Fig. 4(b). It is noted that the intensity of hopping conduction and the diffusion of chemical species are influenced by temperature [11], [16]. However, as a preliminary exploration, the discretisation model proposed here reflects the temperature effects on initial insulation resistivity ρ_0 only (see Table II) and uses the insulation resistivity pattern in Fig. 4(b) to approximate the normalised resistivity variations for all the insulation segments.

III. MODEL RESULTS AND DISCUSSION

A. IR Simulation for Thermal Ageing Only

Figs. 5(a) and 5(b) show the distributions of initial resistivity and degradation rates across insulation segments respectively which are estimated based on the model parameters in Table II combined with the insulation temperature distribution in Fig. 2. The segments in higher temperatures are shown to have smaller initial resistivity but larger degradation rates. This results in the higher-temperature segments having smaller resistances during the thermal ageing process, as shown in Fig. 6(a) or 6(b) for an ageing time of 15 days or 60 days.

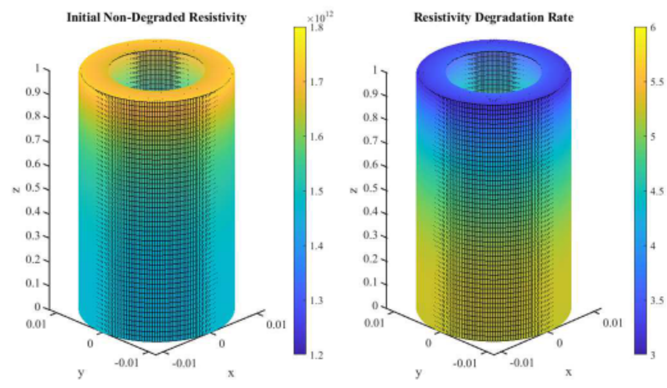

(a) (b)

Fig. 5. Distributions of temperature-dependent (a) initial resistivity (Ω·m) and (b) thermal ageing-related degradation rates (%/day) across insulation segments.

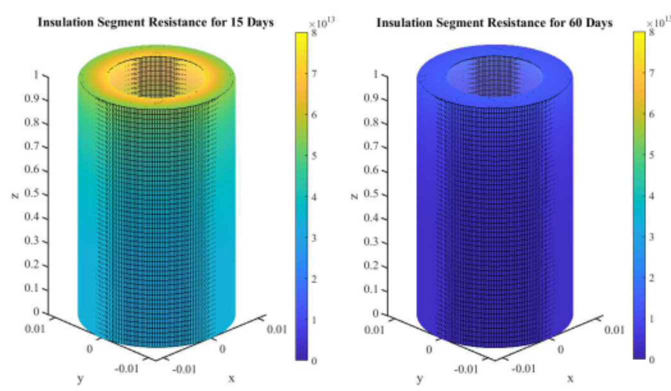

(a) (b)

Fig. 6. Distributions of resistances (Ω) across insulation segments subject to the thermal ageing effect over (a) 15 days and (b) 60 days.

C. IR Simulation for Annealing & Thermal Ageing

The distributions of insulation segment resistances simulated under the joint effects of annealing and thermal ageing over 15 days and 60 days are shown in Figs. 7(a) and 7(b) respectively.

Different from the modelling of the thermal ageing effect which always reduces insulation segment resistances over time, the U-shape variation of insulation resistivity under the joint effects (see Fig. 4(b)) leads to the segment resistances for 60 days being greater than those for 15 days in this case. In the main, the bulk IR modelled under the thermal ageing effect or under the joint effects for up to 90 days exhibits an exponential drop or a U-shape variation respectively. The different IR patterns illustrate the necessity of additionally modelling the annealing effects on IR variations due to the presence of semicon layers.

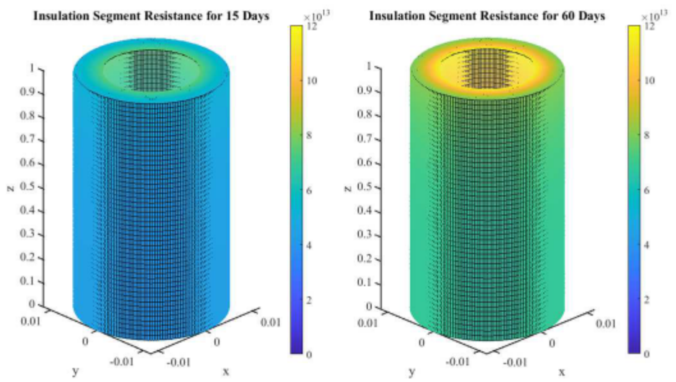

(a) (b)

Fig. 7. Distributions of resistances (Ω) across insulation segments subject to the joint effects of annealing and thermal ageing over (a) 15 days and (b) 60 days.

D. Discussion

The U-shape variation of insulation resistivity modelled here mainly reflects the annealing effect where hopping conduction enhanced by the diffusion of chemical species outweighs band conduction. When heating process goes further, the exhaustion of chemical species will make the band conduction dominant in insulation. Since the gap between valence and conduction bands constantly drops under the thermal ageing effect, an IR decline is expected to follow the U-shape change. Therefore, it might be beneficial to model the effects of annealing or thermal ageing on hopping or band conduction separately and then estimate the equivalent resistivity under the two conduction mechanisms to reflect the joint effects of annealing and thermal ageing with the presence of semicon layers.

IV. Conclusions and Future Work

Cross-linked polyethylene (XLPE) insulated electrical cables operating at elevated temperature undergo both annealing and thermal ageing processes where the insulation resistance (IR) is dominated by the hopping and band conduction respectively. This paper has developed a discretisation model to estimate the temperature distribution across XLPE insulation and simulate the exponential decline of IR under the thermal ageing effect or the U-shape IR variation under the joint effects of annealing and thermal ageing. The discretisation model has been tested based on a particular XLPE insulation sample with the temperature distribution inferred from an artificial neural network combined with the finite volume simulation. The model parameters have been fitted to laboratory measurements of insulation resistivity or conductivity. The IR simulation results indicate the necessity of combining annealing and thermal ageing effects to model IR variations of XLPE insulation in contact with semicon layers.

The discretisation IR model proposed here will be developed further to simulate joint effects of annealing and thermal ageing on IR variations in a physical way, and then fitted to laboratory measurements to understand the characteristics of hopping and band conduction mechanisms in insulation with the presence of semicon layers over the heating process.

Acknowledgment

Part of this research was developed under the UK Engineering and Physical Sciences Research Council grant EP-T001445-1.

References

[1] D. Das-Gupta, "Conduction mechanisms and high-field effects in synthetic insulating polymers," *IEEE Trans. Dielectr. Electr. Insul.*, vol. 4, no. 2, pp. 149-156, Apr. 1997.

[2] F. Aras, V. Alekperov, N. Can, et al., "Aging of 154 kV underground power cable insulation under combined thermal and electrical stresses," *IEEE Electr. Insul. Mag.*, vol. 23, no. 5, pp. 25-33, Sept.-Oct. 2007.

[3] A. Azimuddin and S.S. Refaat, "A comprehensive model for electrical degradation of power cable insulation," in *Proc. 2021 IEEE Conf. Electr. Insul. Dielectr. Phenomena (CEIDP)*, Vancouver, Canada, pp. 133-138.

[4] A.S. Alghamdi and R.K. Desuqi, "A study of expected lifetime of XLPE insulation cables working at elevated temperatures by applying accelerated thermal ageing," *Heliyon*, vol. 6, no. 1, p. e03120, Jan. 2020.

[5] C. Zhou, H. Yi, and X. Dong, "Review of recent research towards power cable life cycle management," *IET High Voltage*, vol. 2, no. 3, pp. 179-187, Sep. 2017.

[6] F. Meng, C. Dai, A. Paramane, et al., "Effect of thermal ageing on insulation properties of 500 kV DC XLPE submarine cable insulation," in *Proc. 2020 IEEE CEIDP*, East Rutherford, NJ, USA, pp. 516-519.

[7] X. Yang, Y. Zhang, H. He, et al., "Influence of thermal ageing on the optimal performance of XLPE cable insulation," in *Proc. 2020 Int. Symp. Electr. Insul. Mater.*, Tokyo, Japan, pp. 502-505.

[8] Y.-S. Chang and A. Mosleh, "Predictive model on the degradation of the electrical resistance of cable insulation," in *Proc. 14th Probabilistic Safety Assessment Manage.*, Los Angeles, CA, USA, 2018, pp. 1-8.

[9] X. Ge, M. Given, and B.G. Stewart, "A power cable thermal aging insulation resistance degradation model," in *Proc. 2022 IEEE Conf. Electr. Insul. Dielectr. Phenomena*, Denver, CO, USA, pp. 53-56.

[10] J.A. Diego, J. Belana, J. Orrit, et al., "Annealing effect on the conductivity of XLPE insulation in power cable," *IEEE Trans. Dielectr. Electr. Insul.*, vol. 18, no. 5, pp. 1554-1561, Oct. 2011.

[11] J. Orrit, "Study on conduction mechanisms of medium voltage cable XLPE insulation in the melting range of temperatures," Ph.D. dissertation, Polytechnic University of Catalonia, Catalonia, Spain, 2011.

[12] M. Stojanović, J. Klimenta, M. Panić, et al., "Thermal aging management of underground power cables in electricity distribution networks: a FEM-based Arrhenius analysis of the hot spot effect," *Electr. Eng.*, vol. 105, pp. 647-662, Apr. 2023.

[13] X. Ge, M. Given, and B.G. Brian, "Determining accelerated aging power cable spatial temperature profiles using Artificial Neural Networks," in *Proc. 2022 IEEE Int. Conf. High Voltage Eng. Appl.*, Chongqing, China, pp. 1-4.

[14] M.Á. Rodríguez-Valverde and M. Tirado-Miranda, "A simpler derivation of the integral formula of electrical resistance," *European J. Physics*, vol. 30, pp. L47-L50, May 2009.

[15] Y. Mecheri, L. Boukezzi, A. Boubakeur, et al., "Dielectric and mechanical behavior of cross-linked polyethylene under thermal aging," in *Proc. 2000 Annu. Rep. Conf. Electr. Insul. Dielectr. Phenomena*, Victoria, BC, Canada, pp. 560-563.

[16] F. Frutos, M. Acedo, M. Mudarra, et al., "Effect of annealing on conductivity in XLPE mid-voltage cable insulation," *J. Electrostatics*, vol. 65, no. 2, pp. 122-131, Feb. 2007.